

# A comparative study on Sn macrosegregation behavior of ternary Al-Sn-Cu alloys prepared by gravity casting and squeeze casting

Ming Xu<sup>1</sup>, \*Yan-guo Yin<sup>1</sup>, Cong-min Li<sup>1</sup>, and Cong-chong Duan<sup>2</sup>

1. College of Mechanical Engineering, Hefei University of Technology, Hefei 230002, China

2. Anhui Yihui New Materials Co., Ltd., Hefei 230000, China

**Abstract:** A comprehensive study on Sn macrosegregation behavior in ternary Al-Sn-Cu alloys was carried out by comparative analysis between gravity casting and squeeze casting samples. The microstructure and Sn distribution of the castings were characterized by metallography, scanning electron microscopy (SEM), energy-dispersive X-ray (EDX) spectroscopy, and a direct reading spectrometer. Results show that there are obvious differences in Sn morphology between gravity casting and squeeze casting alloys. Under squeeze casting condition, the grain size of the casting is smaller and the distribution of  $\beta(\text{Sn})$  is uniform. This effectively reduces the segregation of triangular grain boundary as well as the segregation of Sn. The segregation types of Sn in gravity casting and squeeze casting samples are obviously different. The upper surfaces of gravity casting samples show severe negative segregation, while all the lower surfaces have positive segregation. Compared with gravity casting, squeeze casting solidifies under isostatic pressure. Due to the direct contact between the upper surface of the casting and the mold, the casting solidifies faster under higher undercooling degree and pressure. Consequently, the uniform distribution of Sn reduces the segregation phenomenon on the surface of the casting.

**Keywords:** ternary Al-Sn-Cu alloy; squeeze casting; macrosegregation; mechanism

CLC numbers: TG146.21

Document code: A

Article ID: 1672-6421(2023)01-063-08

## 1 Introduction

Ternary Al-Sn-Cu alloys are widely used in the field of mechanical engineering as self-lubricating bearing materials and have excellent tribological and mechanical properties [1-3]. The soft phase is distributed homogeneously in the aluminum alloy matrix, such as Al-Cu, Al, or Al-Si [4-6], which can be used to produce high-end bearings for automobiles, internal combustion engines, hydraulic gear pumps and other mechanical equipment. However, due to the large density difference between the two immiscible phases, substantial macrosegregation occurs during the alloy solidification process [7-9]. Severe macrosegregation not only reduces the wear resistance of the alloy but also reduces other mechanical properties (such as hardness, tensile strength and elongation),

which affects the application prospects of the alloy. Therefore, researchers have conducted many studies on macrosegregation and the solidification mechanisms of immiscible alloys.

Mirković et al. [10] revealed the complex characteristics of the Al-Sn-Cu phase diagram dominated by ternary liquid separation through thermodynamic modelling and experimental studies and identified three different monotectic reactions in this system, in which small changes in alloy composition can produce significantly different microstructures. Zhai et al. [4] studied the thermodynamic properties and microstructure evolution of ternary Al-10%Cu-x%Sn immiscible alloy systems and systematically measured the vertical phase diagram of Al-10%Cu-x%Sn by differential scanning calorimetry (DSC). The vertical phase diagram of the Al-Cu-Sn alloy at a constant 10%Cu cross section was established, and as Sn content rised, three kinds of liquid separation patterns were observed. In recent years, with the development of materials science in zero-gravity environments, increasing attention has been paid to the solidification of immiscible alloys in microgravity fields and highly intense physical fields.

### \*Yan-guo Yin

Male, Professor. Research interests: Lead-free environment-friendly self-lubricating materials, aviation lightweight materials, critical hydraulic friction pair components.

E-mail: abyin@sina.com

Received: 2022-03-30; Accepted: 2022-12-11

Li et al. [11] successfully prepared a phase separation alloy with the second phase uniformly distributed in the matrix under Tiangong-2 microgravity conditions. Kotadia et al. [12] studied the solidification behavior of Al-Sn-Cu-based immiscible alloys under strong shear, and confirmed that strong melt shear can achieve fine and uniform dispersion of the soft phase without macroscopic separation. Zhai et al. [13] prepared a uniform Al-Sn-Cu ternary immiscible alloy by an orthogonal ultrasonic method and revealed the mechanism of the three-dimensional orthogonal ultrasonic method through simulation and experimental verification.

In summary, the macrosegregation of ternary Al-Sn-Cu alloys was mainly researched under the three conditions of a gravity field, microgravity field and strong physical field. However, there are few reports on the trends and mechanisms of soft phase macrosegregation under a pressure field. Under pressure casting conditions, the types of macrosegregation are obviously diversified [14-19], such as positive macrosegregation, negative macrosegregation, channel macrosegregation, axis macrosegregation, surface macrosegregation and so on [20-25]. The macrosegregation trend and mechanism of the soft phase under a pressure field are indispensable factors in the solidification behavior of immiscible alloys and have important scientific and technical significance. Therefore, the present work studied the Sn macrosegregation behavior of ternary Al-Sn-Cu alloys prepared by squeeze casting and compared to gravity casting.

## 2 Experimental procedure

The Al-Sn-Cu alloys were prepared by melting and mixing commercial-grade aluminum (99.7%) with appropriate additions of 99.99% pure Sn and Cu in a silicon carbide crucible using an electric resistance furnace. The chemical compositions of the alloy are shown in Table 1. In order to avoid the influence of Sn segregation, the initial mass fraction of Sn element in each group was determined by a direct reading spectrometer. Gravity casting and squeeze casting were carried out in this experiment. Under the premise of the same

Table 1: Chemical compositions of Al-Sn-Cu alloy

Composition	Sn	Cu	Fe	Al
wt. %	5	4	<0.2	Bal.

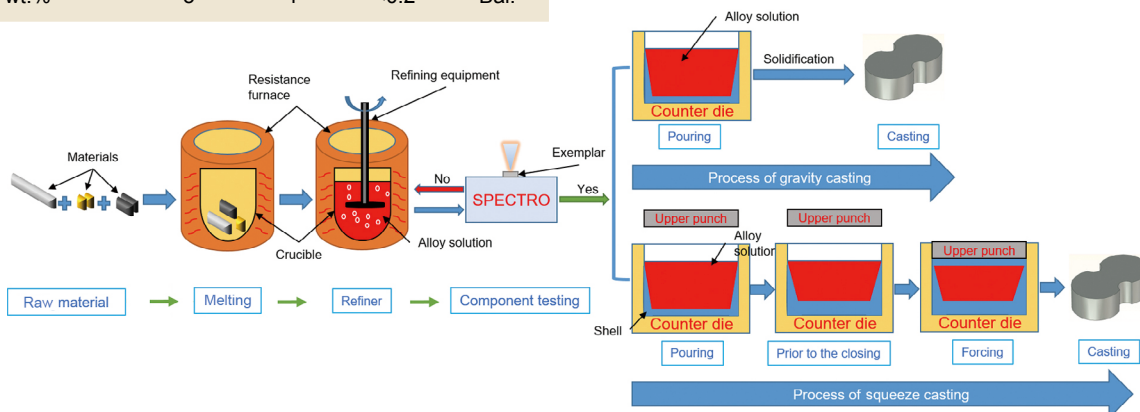


Fig. 1: Schematic illustrations of experimental process for gravity casting and squeeze casting

pouring temperature and mold temperature, the distribution of Sn in castings was detected and analyzed to study the influence of gravity casting and squeeze casting processes on Sn segregation. The lower die of squeeze casting was used as the forming die of the gravity casting. The schematic diagram of the gravity casting and squeeze casting processes is shown in Fig. 1.

Firstly, the material was placed in the silicon carbide crucible and melted in the resistance furnace at 760 °C. Then, the rotary blowing method was used to degas and remove impurities in the liquid aluminum. Finally, the German SPECTRO direct reading spectrometer was used to determine the material composition. The specific shape and size of the sample are shown in Fig. 2. The mold preheating temperature was controlled in the range of 200±10 °C, and the pouring temperature was 700 °C. The casting was solidified under gravity and then removed. The solidification process of squeeze casting was divided into three stages: the first stage was to pour liquid aluminum into the cavity of the lower die (the mold temperature and pouring temperature are consistent with gravity casting); the second stage was the die closing stage, and the closing time was 3 s; the third stage was the solidification process under pressure with a specific pressure of 80 MPa and a holding time of 25 s; and finally the casting was pushed out.

The phase constitutions of the samples were analyzed using the Rigaku D/MAX2500VL/PC rotating target X-ray diffraction (XRD). The second phase of the alloy was analyzed by JSM-6490LV environmental scanning electron microscopy (SEM), and the composition of the alloy was measured by INCA energy dispersive spectroscopy (EDS). The casting was sliced with a wire cutter and marked as the upper surface, 1/4 surface, 1/2 surface, 3/4 surface and lower surface, as shown in Fig. 2(a). Due to the axisymmetric shape of the sample, 5 points on one side were selected for detection and analysis. The detection locations were numbered as points 1-5, as shown in Fig. 2(b). After the surface was polished, the composition of each casting was measured using a German SPECTRO direct reading spectrometer. Each detection position was polished and etched separately as required, and the metallographic structure was observed by a Leica DMI5000M horizontal metallographic microscope.

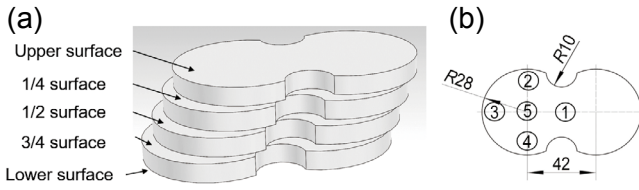


Fig. 2: Schematic diagram of sampling (a) and testing location (b)

### 3 Results and discussion

#### 3.1 Effect of gravity casting and squeeze casting on microstructure

Figure 3 shows the XRD spectra of the Al-Sn-Cu alloy under different casting processes. According to XRD results, both the two samples consist of  $\alpha$ (Al),  $\beta$ (Sn) and  $Al_2Cu$  phases. The change in the formation process does not affect the constitution of the precipitated phase during the solidification of the Al-Sn-Cu alloy, and Sn does not form compounds in the alloy. This is because Sn is immiscible with liquid aluminum during solidification, and it mainly presents a network distribution along grain boundaries in the form of elements, as shown in Fig. 4. The  $\alpha$ (Al) matrix is dark grey,  $\beta$ (Sn) is bright white, and  $Al_2Cu$  compound appears light grey.

Figure 5 shows the microstructures of different surfaces (upper surface, 1/4 surface, 1/2 surface, 3/4 surface, and lower surface) of gravity casting and squeeze casting Al-Sn-Cu alloys at Position 1 in Fig. 2. As shown in Figs. 5(a), (c), (e), (g), and (i), it can be observed that the gravity casting sample grows in the form of dendrites with coarse grains during solidification, and  $\beta$ (Sn) exists in long strips or large blocks, which tends to

segregate at the triangular grain boundaries. Compared with the microstructure of gravity casting, the microstructure of squeeze casting presents fine dendrites. The reduced triangle grain boundaries can be observed, and  $\beta$ (Sn) phase is evenly distributed in the matrix in the form of granular or worm, so that the segregation of  $\beta$ (Sn) is effectively reduced, as shown in Figs. 5(b), (d), (f), (h), and (j). It can be seen from Figs. 5(a) and (b) that the morphology of  $\beta$ (Sn) in the upper surface is significantly different. Compared with the microstructure of the gravity casting, the grains on the upper surface of the squeeze casting are interconnected without complete grain boundaries, and the  $\beta$ (Sn) phase is uniformly distributed in the matrix in granular or worm form. In addition, the microstructure of other surfaces shows an obvious bimodal structure with a mix of coarse and fine dendrites, and the  $\beta$ (Sn) phase size is smaller, and mainly distributes in elliptic or small blocks.

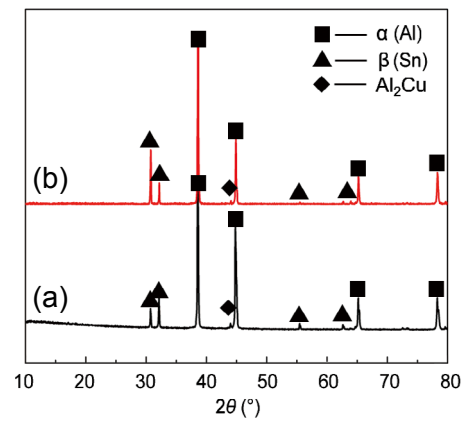


Fig. 3: XRD spectra of alloys in different process states: (a) squeeze casting; (b) gravity casting

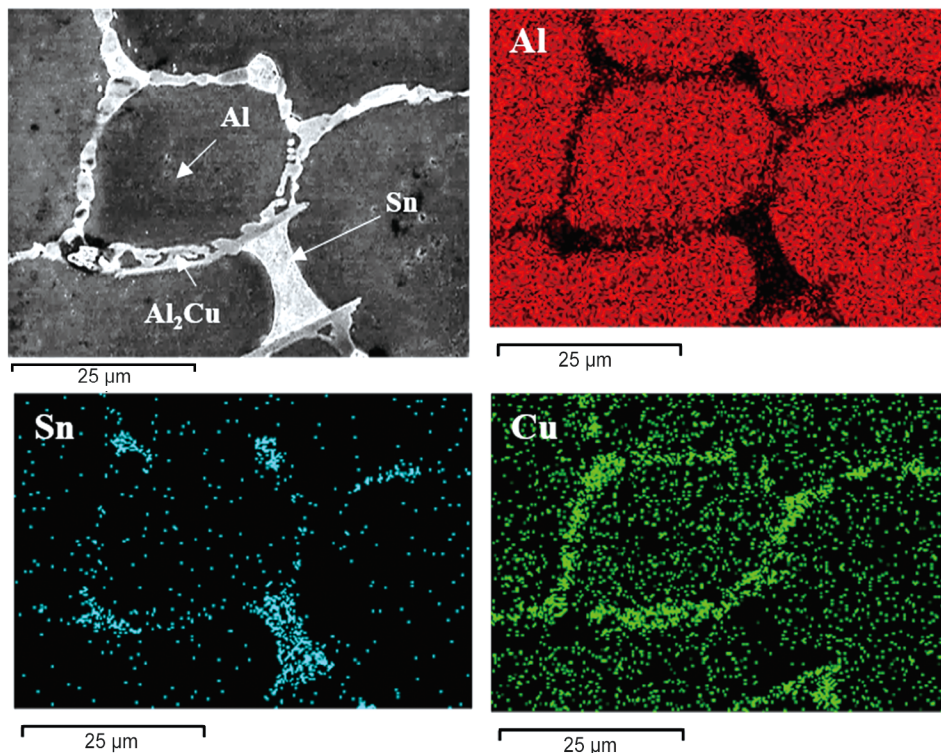


Fig. 4: SEM image and surface scanning composition analysis of gravity casting Al-Sn-Cu alloy

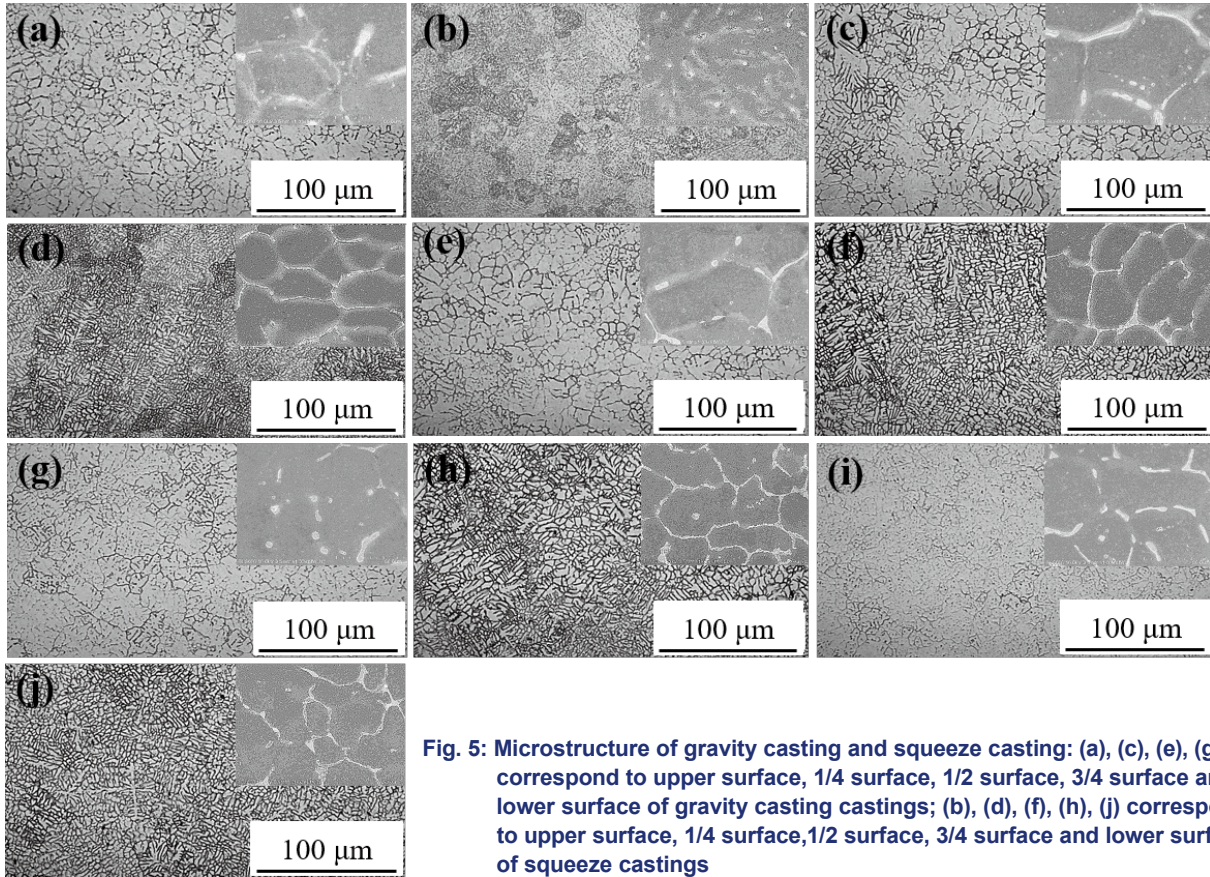


Fig. 5: Microstructure of gravity casting and squeeze casting: (a), (c), (e), (g), (i) correspond to upper surface, 1/4 surface, 1/2 surface, 3/4 surface and lower surface of gravity casting castings; (b), (d), (f), (h), (j) correspond to upper surface, 1/4 surface, 1/2 surface, 3/4 surface and lower surface of squeeze castings

### 3.2 Segregation behavior of Sn in gravity and squeeze casting

The appearance of chemical inhomogeneity in a bulk alloy during the solidification process is known as segregation<sup>[10]</sup>. The segregation rate of Sn element can be calculated by Eq. (1)<sup>[26]</sup>:

$$\eta = \frac{C_i - C_0}{C_0} \quad (1)$$

where  $\eta$  is the segregation rate of a certain part of the casting,  $C_i$  is the Sn mass fraction of the corresponding part of the casting [ $i=1, 2, 3, 4, 5$  corresponding to the positions in Fig. 2(b)], and  $C_0$  is the average Sn mass fraction of the whole casting (original composition mass fraction). When  $\eta=0$ , there is no segregation; when  $\eta<0$ , negative segregation can be observed; when  $\eta>0$ , positive segregation can be observed. To analyze the segregation rate, five detection positions [Fig. 2(b)] were selected on each casting surface to detect composition. The detection results are presented in Table 2. Both positive segregation and negative segregation are observed in gravity casting and squeeze casting samples. In gravity casting, severe negative segregation occurs on the upper surface while positive segregation occurs on the rest surfaces. In contrast, serious positive segregation appears on the lower surface in squeeze casting, while negative segregation is observed on the rest parts, and the segregation degree in the middle region is relatively slight. It can be seen that different forming processes of castings can have a significant effect on the type of segregation. The results show that the segregation degree of Sn in the gravity casting process is greater. In addition, the distribution of Sn elements on different surfaces of the castings

was analyzed. The results in Fig. 6 show that the Sn mass fraction on each surface of gravity castings exhibits obvious fluctuation. In other words, there is serious segregation of Sn on the same surface. Compared with the results of gravity casting, the fluctuation of Sn mass fraction on each surface in squeeze casting is smaller. The upper surface of the casting is basically consistent, indicating that the local segregation phenomenon is significantly improved.

### 3.3 Discussion

During the solidification process of Al-Sn-Cu alloy, the three modes of liquid phase separation among  $\alpha(\text{Al})$ ,  $\beta(\text{Sn})$ , and  $\text{Al}_2\text{Cu}$  can be changed with the increase of Sn mass fraction. According to the phase diagram of Al-Sn-Cu ternary alloy<sup>[4]</sup> shown in Fig. 7, the liquid phase separation and precipitation process of molten Al-Sn-Cu alloy during cooling were studied, as shown in Fig. 8. At the beginning of solidification, the primary  $\alpha(\text{Al})$  phase precipitates from the aluminum liquid. Along with the cooling, the  $\alpha(\text{Al})$  phase grows gradually, and the  $\text{Al}_2\text{Cu}$  phase precipitates along the grown  $\alpha(\text{Al})$  phase, presenting a flat shape. Then, a monotectic reaction occurs in the liquid phase  $L_1 \rightarrow L_2 + \alpha(\text{Al}) + \theta(\text{Al}_2\text{Cu})$ , in which  $L_2$  represents the Sn-rich liquid droplets. Finally, a eutectic reaction occurs in the Sn-rich liquid droplets  $L_2 \rightarrow \alpha(\text{Al}) + \theta(\text{Al}_2\text{Cu}) + \beta(\text{Sn})$ . It is generally believed that the direct influence of composition distribution on the solidified structure is due to the redistribution of the solute between solid and liquid phases<sup>[27]</sup>. According to the phase diagram of Al-Sn binary alloy, Al and Sn are basically insoluble. Thus, the

Table 2: Detection results of Sn at different positions of castings by different processes (mass fraction)

Process	Sampling location	C <sub>0</sub>	Detecting position					Segregation rate, $\eta$ (%)	Segregation type
			C <sub>1</sub>	C <sub>2</sub>	C <sub>3</sub>	C <sub>4</sub>	C <sub>5</sub>		
Gravity casting	Upper surface		4.60	4.34	4.40	4.50	5.07	-21.29	Negative
	1/4 surface		5.90	6.57	6.23	6.29	5.84	5.89	Positive
	1/2 surface	5.82	6.43	6.12	6.02	6.06	5.60	3.83	Positive
	3/4 surface		6.25	5.75	6.22	5.99	6.51	5.53	Positive
	Lower surface		5.98	6.29	6.01	6.26	6.33	6.07	Positive
Squeeze casting	Upper surface		3.86	4.02	3.99	4.00	3.98	-7.05	Negative
	1/4 surface		4.14	4.08	4.59	3.99	4.07	-2.25	Negative
	1/2 surface	4.27	4.36	4.33	4.25	4.29	4.01	-0.56	Negative
	3/4 surface		3.96	3.74	4.32	4.20	4.10	-4.87	Negative
	Lower surface		4.90	4.73	5.02	4.83	5.01	14.73	Positive

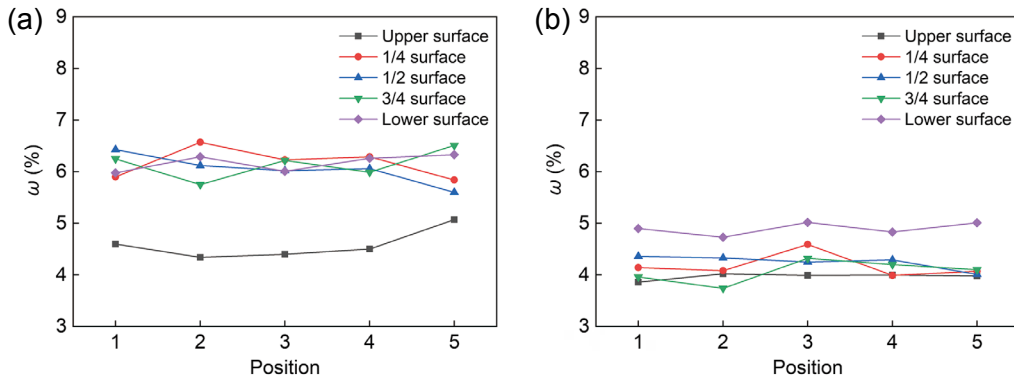


Fig. 6: Mass fraction of Sn on each surface of castings by different processes: (a) gravity casting; (b) squeeze casting

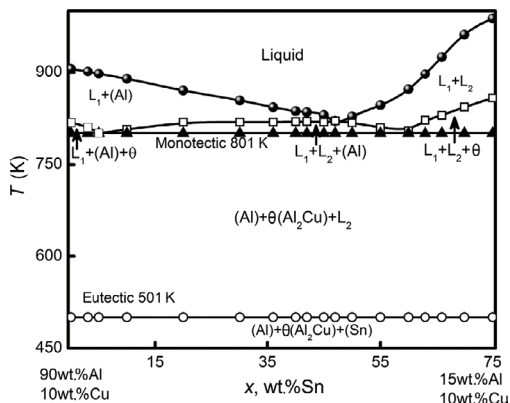


Fig. 7: Vertical phase diagram of ternary Al-Cu-x%Sn alloys at constant 10% Cu determined by DSC method [4]

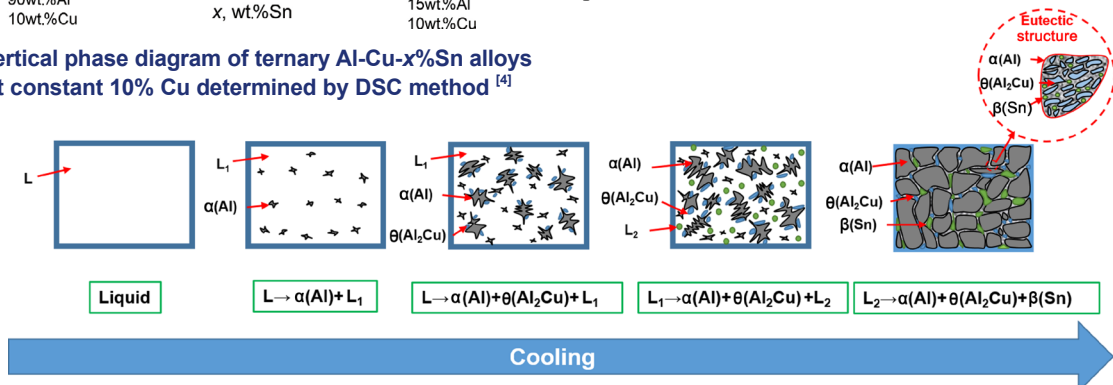


Fig. 8: Diagram of solidification process of Al-Sn-Cu alloy

distribution law of Sn cannot be applied to solute redistribution theory in this case. However, in addition to the influence of solute element redistribution, the flow of the liquid phase plays a vital role in the macrosegregation during solidification [28]. Therefore, the Sn segregation in the casting is closely related to the flow of the Sn-rich liquid droplets. The forces that can lead to liquid flow can be summarized as the solidification shrinkage of the alloy, natural convection, forced flow under the influence of external forces, etc. Besides, the forces of liquid flow can be different according to the different casting processes.

During the process of gravity casting, Al-Sn-Cu alloy is poured into the lower mold cavity, and the surface contacted with the mold cavity rapidly solidifies. The Sn-rich liquid droplets discharge from solidification uniformly dissociate in the liquid phase under the action of pouring momentum. On the one hand, the Sn-rich liquid droplets are discharged after solidification and growth. On the other hand, with the large temperature gradient of the hot nodes at the side, upper and middle portions, the Sn-rich liquid droplets move towards the middle hot node due to the action of the Marangoni effect. As a result, the Sn-rich liquid droplets at the side and upper parts move towards the middle and lower parts under the action of the resultant force. The Sn-rich liquid droplets at the central hot node migrate downward under the influence of both Stokes motion and Marangoni effect, as shown in Fig. 9.

The Sn-rich liquid droplets constantly merge, collide, and grow up under the action of movement. According to Stokes motion and Marangoni effect equation, when the radius of liquid phase is  $r$ , the liquid phase movement velocity  $U_s$  (Stokes motion) and  $U_m$  (Marangoni) can be calculated according to Eqs. (2) and (3) [29, 30].

$$U_s = \frac{2g\Delta\rho(\eta + \eta')}{3\eta(2\eta + 3\eta')}r^2 \quad (2)$$

$$U_m = \frac{2\left|\frac{dT}{dx}\right|\left|\frac{d\alpha}{dT}\right|k}{(2\eta + 3\eta')(2k + k')}r \quad (3)$$

where  $\eta$  and  $\eta'$  are the liquid viscosity values of matrix and liquid phase,  $\Delta\rho$  is the density difference between matrix and liquid phase,  $k$  and  $k'$  are the thermal conductivity of matrix and liquid phase, respectively. In addition,  $dT/dx$  stands for the temperature gradient; while  $da/dT$  is the temperature change of the interfacial energy between the two liquid phases, and  $g$  is the gravitational acceleration. Zhai et al. [13] estimated and studied the velocity of Sn droplets in an Al-Sn-Cu ternary alloy under static condition using Stokes motion and the Marangoni effect, the result is illustrated in Fig. 10, where the radius of the Sn-rich droplet is considered to be from 0 to 30  $\mu\text{m}$  and the moving velocity under Stokes motion and the Marangoni effect is from 0 to  $4.0 \times 10^{-3} \text{ m}\cdot\text{s}^{-1}$  and 0 to  $6.3 \times 10^{-5} \text{ m}\cdot\text{s}^{-1}$ , respectively. As can be observed, Stokes motion is two orders

of magnitude greater than Marangoni effect, implying that Stokes motion is dominant in Sn droplet movement under static solidification conditions.

In the process of gravity casting, the liquid flow is mainly driven by solidification shrinkage and natural flow, among which the natural flow mainly comes from Stokes motion and Marangoni effect. According to the preceding findings [13], Stokes motion is important in the macroscopic segregation of Sn. Moreover, under the effect of Stokes motion, the Sn-rich liquid droplets mostly flow towards the lower regions of the casting throughout the solidification process. Since liquid aluminum encounters the solidification procedure from bottom to top, the higher section gives enough movement time for Sn-rich droplets. As a result, the mass fraction of Sn on the upper surface is low, while the mass fraction of Sn on the lower surface is high, resulting in negative segregation on the upper surface and positive segregation on the lower. The remaining liquid droplets lose their fluidity as the dendritic skeleton is built, and the Sn-rich droplets complement the solidified body under the influence of negative pressure caused by solidification shrinkage. The trend of negative segregation on the upper and positive segregation on the lower surfaces is intensified by the sequence of bulk shrinkage from bottom to top, which follows the solidification sequence from bottom to top. Among them, due to direct contact with the mold on the lower surface, the degree of undercooling is large and the solidification process is fast. The excluded Sn-rich liquid droplets are quickly fixed due to poor mobility. In addition, the negative pressure generated by solidification shrinkage induces the remaining liquid phase to continuously complement the

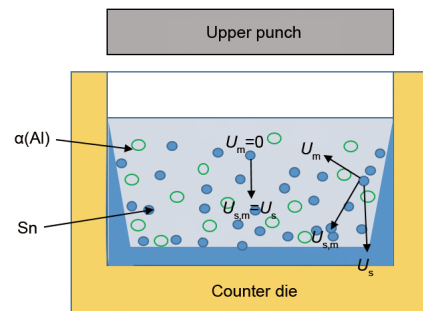


Fig. 9: Movement direction of Sn liquid phase under Stokes motion and Marangoni effect

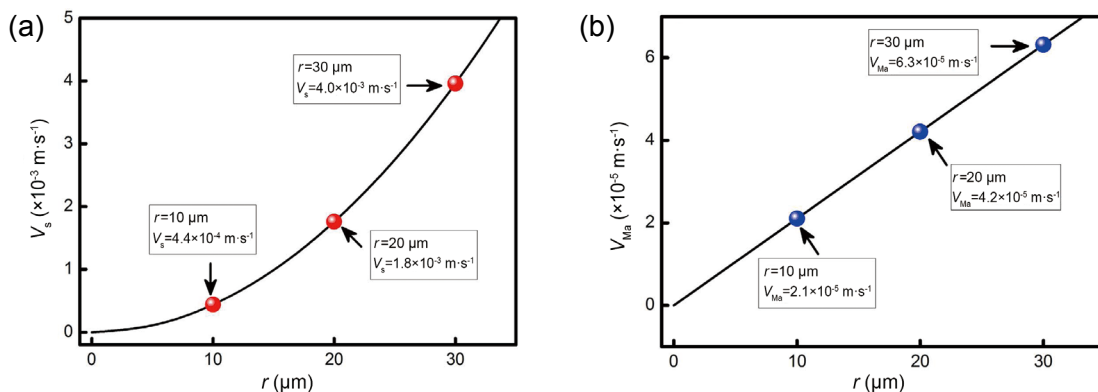


Fig. 10: Stokes motion and Marangoni motion velocities of secondary (Sn) droplets: (a) Stokes motion; (b) Marangoni motion [13]

solidified body, resulting in a higher Sn mass fraction on the lower surface and the maximum positive segregation degree.

Compared with gravity casting, squeeze casting is formed under isostatic pressure. Therefore, besides solidification shrinkage and natural convection, liquid flow under pressure is the main factor of Sn segregation. The liquid aluminum is initially poured into the bottom die cavity during the squeeze casting process. Before the mold is closed, the Sn-rich droplets continue to converge downward, mostly due to Stokes motion, which lowers the upper Sn mass fraction and raises the lower Sn mass fraction. This circumstance is consistent with the Sn segregation distribution of gravity casting. The top part segregation degree is proportional to the mold fitting time. The longer the mold fitting time, the more intense the movement of the Sn-rich droplets in the top region caused by Stokes motion, and the greater the segregation degree. The top surface segregation degree is high under the experimental circumstances, where the mold fitting time is 3 s and the radius of the Sn-rich droplet is from 0 to 30 μm and the moving distance under Stokes motion is from 0 to 1.2×10<sup>-2</sup> m<sup>[13]</sup>. The liquid aluminum is solidified under pressure when the mold is closed. According to Clausius-Clapeyron Eq. (4)<sup>[31]</sup>:

$$\frac{\Delta T_f}{\Delta p} = \frac{T_f(V_L - V_S)}{\Delta H_f} \quad (4)$$

where  $T_f$  is the equilibrium solidification temperature of the alloy;  $V_L$  is the liquid phase volume of alloy;  $V_S$  is the solid phase volume of alloy;  $\Delta H_f$  is the change of the latent heat of melting;  $\Delta p$  is the change of pressure on the alloy. Based on the Eq. (4), with the increase of pressure, the equilibrium solidification temperature  $T_f$  increases, the solidification rate accelerates, and the grain size of the casting significantly decreases compared with that of the gravity casting (as shown in Fig. 5). According to Wang et al.<sup>[32]</sup>, the pressure loss rate of aluminum alloy during the squeeze casting process is around 41%, and the pressure from the top surface to the lower surface alters in a gradient. The solidification sequence should follow the same trend as the pressure gradient, according to Eq. (4). However, since direct contact with the mold's bottom surface gives a higher level of undercooling, even if the pressure is low, the solidification rate is higher. As a result, squeeze casting solidifies from the top and lower surfaces to the central surface. Among them, the top die immediately touches the upper surface of the casting, and the higher degree of undercooling and pressure cause a rapid solidification at the casting's upper surface. As a result, the excluded Sn has no time to migrate, coagulate, or mature. The mass fraction of Sn remains almost constant before and after the mold is closed. As a result, there is significant negative segregation, and the microstructure is satisfactory with a rather uniform Sn distribution, as shown in Fig. 5(b). On the one hand, the lower surface is preferentially solidified before the mold is closed. The negative pressure generated by solidification shrinkage causes Sn-rich liquid droplets on 3/4 surface to continuously feed the lower surface, resulting in a high Sn mass fraction on

the lower surface. When the mold is closed, the pressure drives the Sn-rich liquid droplets into the feeding channel, increasing the Sn mass fraction of the lower surface even more.

At the late solidification stage, the dendrite skeleton is formed quickly, and the Sn-rich liquid droplets lose its fluidity. The results of Flemings's study showed that in a wide range of solid phase fraction variation, the flow of liquid droplets between dendrites could be described by Darcy's Law [Eq. (5)], the basic law of fluid flow in porous media<sup>[33]</sup>:

$$v_x = -\frac{Kdp}{\mu g_L dx} \quad (5)$$

where  $v_x$  is the flow rate of the liquid phase in the interdendrite;  $k$  is the permeability coefficient;  $\mu$  is the viscosity of the liquid phase;  $g_L$  is the mass fraction of the liquid phase;  $dp/dx$  is the pressure gradient. According to Eq. (5), in the pressure field, the flow rate of the liquid phase in the dendrite is proportional to the pressure. In other words, the pressure will greatly increase the flow rate of the Sn-rich liquid droplets in the interdendrite, resulting in the generation of Sn segregation. As the pressure differential from upper surface to lower surface varies, so does the flow velocity of Sn-rich droplets in the interdendrite. Droplets containing Sn flow from the 1/4 surface to the lower surface. The flow velocity from 1/4 surface to 1/2 surface is quicker than the flow velocity from 1/2 surface to 3/4 surface. As a consequence, 1/4 surface has significant negative segregation whereas 1/2 surface has minimal negative segregation. The Sn-rich droplets on 3/4 surface not only seep downward under pressure, but also reinforce the lower surface during the early stage of solidification, resulting in a high degree of negative segregation. Simultaneously, the segregation degree of the lower surface is increased, resulting in significant positive segregation on the lower surface, as seen in Table 2.

## 4 Conclusions

(1) The microstructure of gravity casting is obviously different from that of squeeze casting. Under the squeeze casting process, the grain size of the casting is smaller and the distribution of  $\beta(\text{Sn})$  is uniform, reducing the segregation of triangular grain boundary and effectively improving the segregation of Sn.

(2) There is a significant difference between the gravity casting and the squeeze casting in the Sn segregation type. The upper surface of the gravity castings shows severe negative segregation, and all the lower surfaces exhibit positive segregation. However, the lower surface of the squeeze casting has positive segregation, while the other surfaces show negative segregation.

(3) Compared with gravity castings, squeeze castings solidify under isostatic pressure. Due to the direct contact between the upper surface and the die, the solidification rate of the casting is faster under the action of higher undercooling degree and pressure, and Sn distribution is uniform, resulting in reduction of segregation on the surface of the casting.

## Acknowledgements

This research was financially supported by the National Natural Science Foundation of China (No. 51575151) and the Science and Technology Project of Anhui Province, China (No. 1501021006).

## Conflict of interest

The authors declare that they have no conflict of interest.

## References

- [1] Ratke L, Diefenbach S. Liquid immiscible alloys. *Materials Science and Engineering*, 1995, 15R: 263–347.
- [2] Ratke L. *Immiscible liquid metals and organic*. Germany: DGM Informations GmbH, 1993: 199–258.
- [3] Davis J R. *Aluminum and aluminum alloys*. ASM International, 1993: 351–416.
- [4] Zhai W, Hu L, Geng D L, et al. Thermodynamic properties and microstructure evolution of ternary Al-10%Cu-x%Sn immiscible alloys. *Journal of Alloys and Compounds*, 2015, 627: 402–409.
- [5] Kaban, Curiotto I, Chatain S, et al. Surfaces, interfaces and phase transitions in Al-In monotectic alloys. *Acta Materialia*, 2010, 58: 3406–3414.
- [6] Fang X W, Fan Z Y. Rheo-diecasting of Al-Si-Pb immiscible alloy. *Scripta Materialia*, 2006, 54: 789–793.
- [7] Bertelli F, Brito C, Ferrdira I L, et al. Cooling thermal parameters, microstructure, segregation and hardness in directionally solidified Al-Sn-(Si, Cu) alloys. *Materials and Design*, 2015, 72: 31–42.
- [8] Yan Y J, Wei C, He Y X, et al. Effect of high magnetic field on solidification microstructure evolution of a Cu-Fe immiscible alloy. *China Foundry*, 2022, 19(4): 335–341.
- [9] Wang F, Choudhury A, Selzer M, et al. Effect of solutal Marangoni convection on motion, coarsening, and coalescence of droplets in a monotectic system. *Physical Review E*, 2012, 86(6-2): 066318.
- [10] Mirković D, Grobner J, Schmid-Fetzer R. Liquid demixing and microstructure formation in ternary Al-Sn-Cu alloys. *Materials Science and Engineering A*, 2008, 487: 456–467.
- [11] Li W, Jiang H X, Zhang L L, et al. Solidification of Al-Bi-Sn immiscible alloy under microgravity conditions of space. *Scripta Materialia*, 2019, 162: 426–431.
- [12] Kotadia H R, Doernberg E, Patel J B, et al. Solidification of Al-Sn-Cu based immiscible alloys under intense shearing. *Metallurgical and Materials Transactions A*, 2009, 40: 2202–2211.
- [13] Zhai W, Wang B J, Hu L Z, et al. Three orthogonal ultrasounds fabricate uniform ternary Al-Sn-Cu immiscible alloy. *Scientific Reports*, 2016, 6(1): 36718.
- [14] Guo K L, Xin X R, Liu T. Calculation method study on closing die radial extrusion force off floating die. *Forging & Stamping Technology*, 2010, 35(1): 70–74. (In Chinese)
- [15] Kim H H, Kang C G. Numerical simulation and experimental study for rheo-forged component using direct and indirect die system. *Transactions of Nonferrous Metals Society of China (English)*, 2010, 20(9): 1799–1804.
- [16] Zhang H Y, Xing S M, Zhang Q H. Evaluation of the mold-filling ability of alloy melt in squeeze casting. *Journal of University of Science and Technology Beijing: Mineral Metallurgy Materials (Eng. Ed.)*, 2006, 13(1): 60–66.
- [17] Zhang X L, Wang T M, Li T J, et al. Numerical study on rheocasting A356 alloy using cooling slope method. *The 7th Pacific Rim International Conference on Modeling of Casting and Solidification Process (MCSP7-2007)*, Dalian, 2007: 643–648.
- [18] Yang X R, Xu X D, Liu P. Effect of vertical bending pouring channel on the microstructure of semisolid state A356 alloy feed stock. *Shanxi Metallurgy*, 2013, 36: 14–17. (In Chinese)
- [19] Yang X R, Sun B Y, Huang Q X, et al. Preparation of semisolid feedstock by reversed cone channel pouring. *Advanced Materials Research*, 2012, 535-537: 2606–2609.
- [20] Guo H M, Yang X J, Hu B. Low superheat pouring with a shear field in rheocasting of aluminum alloys. *Journal of Wuhan University of Technology - Materials Science Edition*, 2008, 23: 54–59.
- [21] Li X M, Wang Y, Bi Q C. Experimental study on gas bubble rising velocity in different liquids. *Journal of Xi'an Jiaotong University*, 2003, 37: 971–974.
- [22] Liu W, Xing S M, Bao P W. Energy dissipation and apparent viscosity of semisolid metal during rheological processes Part II: Apparent viscosity. *Journal of Materials Science and Technology*, 2007, 23: 801–805.
- [23] Liu W, Xing S M, Bao P W, et al. Energy dissipation and apparent viscosity of semisolid metal during rheological processes Part I: Energy dissipation. *Journal of Materials Science & Technology*, 2007, 23(3): 342–346.
- [24] Zhong Y, Yan D S, Su G Y, et al. Microsegregation and improvement of LY12 alloy by squeeze casting. *Acta Metallurgica Sinica*, 2001, 37(1): 42–46. (In Chinese)
- [25] Chen F Y, Jie W Q. Experimental study on microstructure segregation of Al-Cu-Zn Alloy and Scheil Model. *Acta Metallurgica Sinica*, 2004, 40(6): 664–668.
- [26] Jie W Q, Zhou Y H. Formation of hot-top segregation in steel ingot and effect of steel compositions. *Metallurgical and Materials Transactions B*, 1989, 5(20): 723–730.
- [27] Liu J L, Zhao Y Q, Zhou L. Segregation of Ti-2.5Cu, Ti-3Fe and Ti-3Cr alloy ingot. *Rare Metal Materials and Engineering*, 2004, 33(7): 731–735.
- [28] Lee S G, Patel G R, Gokhale A M. Inverse surface macrosegregation in high-pressured die-cast AM60 magnesium alloy and its effects on fatigue behavior. *Scripta Materialia*, 2005, 52(10): 1063–1068.
- [29] Lappa M. *Fluids, materials, and microgravity-numerical techniques and insights into physics*. Oxford: Elsevier Ltd., 2004.
- [30] Young N O, Goldstein J S, Block M J. *Journal of Fluid Mechanics*, 1959, 6: 350–356.
- [31] Ghomashchi M R, Vikhrov A. Squeeze casting: An overview. *Journal of Materials Processing Technology*, 2000, 101(1–3): 1–9.
- [32] Wang F F, Ma Q X, Meng W, et al. Experimental study on the heat transfer behavior and contact pressure at the casting-mold interface in squeeze casting of aluminum alloy. *International Journal of Heat and Mass Transfer*, 2017, 112: 1032–1043.
- [33] Flemings M C. Our understanding of macrosegregation past and present. *ISIJ International*, 2000, 40(9): 833–841.